JOURNAL OF MATERIALS SCIENCE **40** (2005) 909–917

Processing by equal-channel angular pressing: Applications to grain boundary engineering

MINORU FURUKAWA
Department of Technology, Fukuoka University of Education, Munakata, Fukuoka 811-4192, Japan

ZENJI HORITA
Department of Materials Science and Engineering, Faculty of Engineering, Kyushu University, Fukuoka 812-8581, Japan

TERENCE G. LANGDON*
Departments of Aerospace & Mechanical Engineering and Materials Science, University of Southern California, Los Angeles, CA 90089-1453, USA
E-mail: langdon@usc.edu

Equal-channel angular pressing (ECAP) is a processing technique in which a sample is pressed through a die constrained within a channel so that an intense strain is imposed without incurring any change in the cross-sectional dimensions of the sample. This procedure may be used to achieve considerable grain refinement in pure metals and metallic alloys with as-pressed grain sizes lying typically within the submicrometer range. Careful experiments reveal only a minor change in the grain size with increasing numbers of passes through an ECAP die but there is a significant change in the distribution of grain boundary misorientations as a function of the total imposed strain. In practice, the microstructure evolves with increasing strain from an array of grains where the boundaries are predominantly in low-angle misorientations to an array of grains where a high fraction (typically $\geq$60%) is in high-angle misorientations. This evolution has a significant effect on the characteristics of the as-pressed materials including the high temperature mechanical properties and the measured rates of diffusion. In addition, the evolution provides an opportunity to use Grain Boundary Engineering in order to optimize the behavior of the material.

1. Introduction

Approximately one hundred years ago, at the turn of the last century, there was lively scientific debate in the field then known as metallurgy concerning the nature and significance of the boundaries or interfaces that had been clearly resolved in polycrystalline samples through the use of simple bench-top optical microscopes. There were two strong and opposing viewpoints proposing that these interfaces were either an amorphous layer or that they were crystalline and represented simply "the meeting of one grain with another" [1]. McLean [2] subsequently summarized much of this fascinating debate in the opening chapter of his classic book, published in 1957, which dealt exclusively and for the first time with the characteristics of grain boundaries and with the gradual development of our understanding of the role played by these boundaries in dictating the physical and mechanical characteristics of all polycrystalline materials.

Building on this accumulated knowledge, a significant development occurred almost two decades ago when Watanabe [3] introduced a new and bold initiative termed "Grain Boundary Design" in which it was proposed that specific beneficial properties, such as high strength and good ductility, may be attained through a close control of the nature of the grain boundary character distributions. Thus, for example, recognizing that low-angle grain boundaries and coincidence boundaries tend to be reasonably resistant to intergranular fracture but random high-angle grain boundaries are generally preferential sites for crack nucleation and growth, it follows that an optimum condition may be achieved through employing grain boundary design and ensuring that any selected material contains an unusually high fraction of low-angle and coincidence boundaries. This novel concept provided a significant impetus for detailed studies into the factors influencing the grain boundary character distributions in polycrystalline materials but the approach was hampered, at least initially, by the relatively limited availability of appropriate analytical facilities and especially by the time-consuming nature of any detailed and statistically

*Author to whom all correspondence should be addressed.

valid analysis of grain boundary misorientations and distributions.

Grain Boundary Design has more recently evolved into the concept of Grain Boundary Engineering in which boundaries are engineered, or tailored, for use in specific applications. In addition, the concept has benefited significantly from the recent widespread introduction of powerful new tools, such as orientation imaging microscopy (OIM), where computer-aided scans may be conducted fairly quickly and efficiently to provide detailed misorientation profiles and microstructural information over extensive areas of polycrystalline samples incorporating large numbers of grains. Recent reviews summarize some of these more recent developments [4, 5].

Numerous experiments have shown that it is often possible to change the distributions of grain boundary misorientations through the use of appropriate heat treatments. This approach was applied, for example, to rapidly solidified and annealed Fe-Si ribbons [6] and to Ni alloys where the presence of high fractions of low-angle boundaries leads to a significant improvement in the susceptibility of these alloys to intergranular stress corrosion cracking [7, 8]. More recent investigations have shown that the presence of external magnetic fields may alter the grain boundary character distributions produced during the annealing process and experimental results demonstrate that increases in the strength of the magnetic field lead to corresponding increases in the fractions of low-angle boundaries having misorientations of less than 15° [9, 10]. Techniques involving annealing and magnetic annealing are therefore attractive procedures in any attempts to maximize the beneficial properties attained through the judicious use of grain boundary engineering.

The objective of the present paper is to present an alternative approach in which different grain boundary character distributions are achieved not through an annealing process but through the application of severe plastic deformation (SPD). Processing by SPD has attracted much attention over the last five years because it provides the capability of producing bulk materials that have exceptionally small grain sizes in the submicrometer or even in the nanometer range [11, 12]. The basic principle of SPD processing is that a material is subjected to a very large strain but this strain is attained without any concomitant change in the overall dimensions of the sample. Thus, SPD processing differs in a very significant way from more conventional processing techniques such as extrusion, rolling and drawing where the introduction of strain is associated with a reduction in the cross-sectional area of the work-piece.

There are two principle techniques for SPD processing: Equal-Channel Angular Pressing (ECAP) in which a sample is subjected to a shearing strain as it passes through a die [13–16] and High-Pressure Torsion (HPT) in which material is subjected to a high pressure and concurrent torsional straining [17, 18]. In practice, however, HPT employs small samples in the form of disks whereas ECAP uses reasonably large billets and the process may be scaled-up to produce bulk samples suitable for use in industrial applications [19]. This paper is therefore concerned with processing by ECAP and the principle of this technique is described in the following section. The next sections describe the microstructures produced in processing by ECAP and the relevance and application of this technique to Grain Boundary Engineering.

2. Principle of equal-channel angular pressing

The principle of ECAP is illustrated schematically in Fig. 1. A die is constructed containing an internal channel that is bent through an abrupt angle usually equal to, or very close to, 90°. The sample is machined to fit within the channel and it is then pressed through the die using a plunger. An intense shear strain is therefore imposed as the sample passes through the shearing plane at the intersection of the two parts of the channel and the sample subsequently emerges from the die having the same cross-sectional dimensions. Three orthogonal planes are defined in Fig. 1: the X or transverse plane perpendicular to the direction of flow, the Y or flow plane parallel to the side face at the point of exit from the die and the Z or longitudinal plane parallel to the top face at the point of exit from the die. Since the cross-sectional dimensions remain unchanged during passage through the die, the same sample may be pressed repetitively to accumulate a very large total strain. The precise strain imposed in each pass through the die is dictated primarily by the angle between the two parts of the channel (90° in Fig. 1) but also to a lesser extent by the outer angle of curvature at the point where the two parts of the channel intersect (0° in Fig. 1). For a die having a channel bent through an angle of 90°, it can be shown from first principles that the imposed strain in each pass is approximately equal to 1 [20].

In practice, it is apparent that different shearing planes may be activated within the sample by rotating the billet between each separate pass [14] and this has led to the development of four separate and distinct processing routes. These four routes are termed A, B_A, B_C and C and they represent situations in which

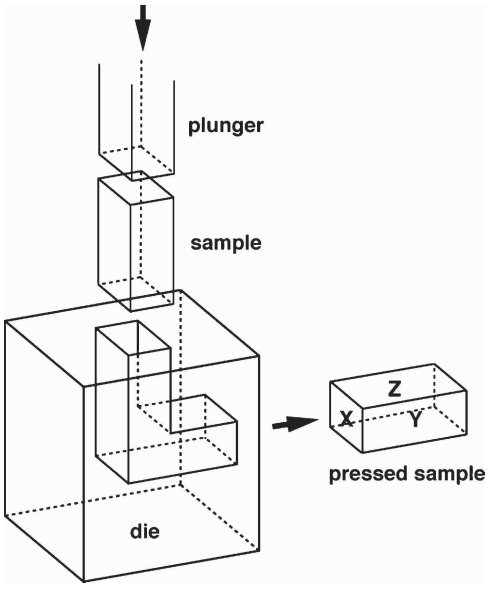

Figure 1 Schematic illustration of ECAP.

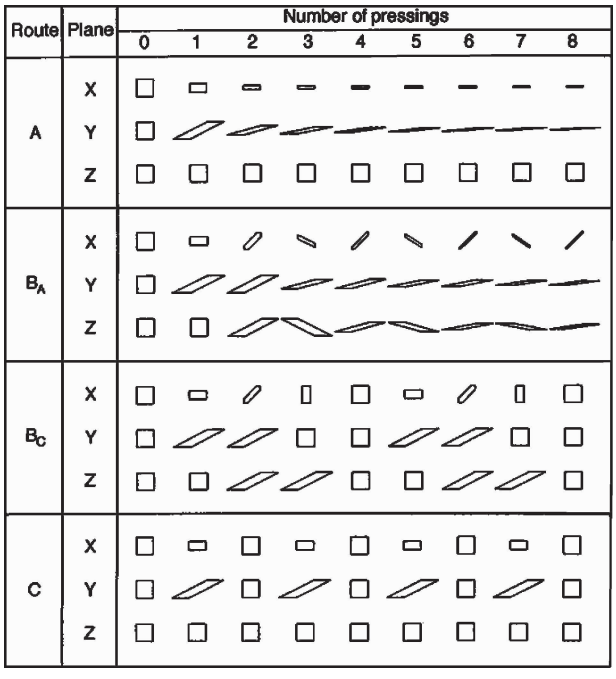

Figure 2 Distortions associated with a cubic element when viewed on the X, Y and Z planes for 1 to 8 passes using processing routes A, B_A, B_C and C [21].

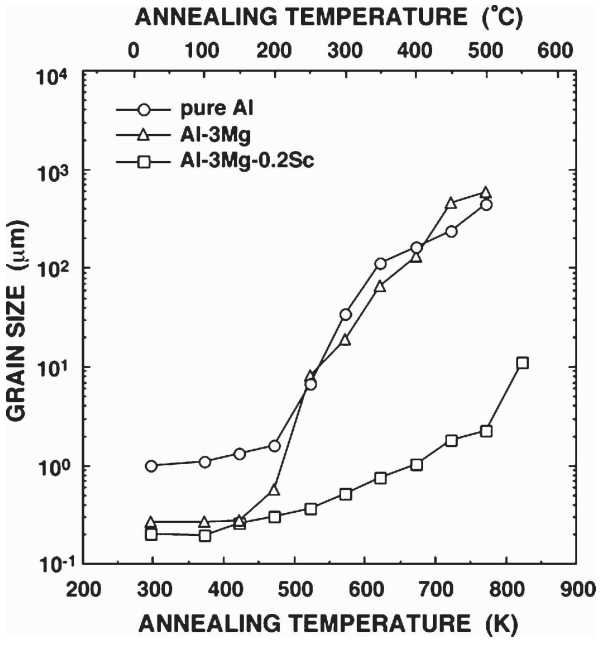

Figure 3 Variation of the as-pressed grain size with annealing temperature for pure Al [26], an Al-3% Mg alloy [26] and an Al-3% Mg-0.2% Sc alloy [27].

the sample is not rotated between passes (route A), rotated by 90° in alternate directions between each pass (route B_A), rotated by 90° in the same sense between passes (route B_C) and rotated by 180° between passes (route C). Fig. 2 illustrates the distortion of a simple cubic element when pressed through a die for up to a total of 8 passes using these four processing routes: for each route the shape of the cube is illustrated separately for the X, Y and Z planes [21]. Thus, routes A and B_A give an increasing distortion of the cube with additional passes but in routes B_C and C the cubic element is restored after every 4 and 2 passes, respectively. In addition, deformation occurs on all three planes when using route B_C but there is no deformation in the Z plane when using route C. As a consequence of these characteristics and the documented shearing patterns for each processing route [22], it is found experimentally that route B_C is the optimum processing route in order to achieve a homogeneous array of ultrafine grains separated by boundaries having high angles of misorientation [23].

3. The microstructures produced using ECAP

Processing by ECAP imposes a very high strain on the sample and thus a very large number of dislocations are introduced into the material. After a single pass the microstructure consists of bands of elongated subgrains with the boundaries having low angles of misorientation, but with subsequent passes the microstructure evolves gradually into an array of ultrafine and essentially equiaxed grains separated by high-angle grain boundaries [24, 25]. This gradual evolution is thus the key to attaining different grain boundary character distributions through ECAP.

Although ultrafine grains are produced through ECAP processing, nevertheless these grains are only retained at elevated temperatures in the presence of precipitates that serve to inhibit grain growth. Fig. 3 shows the variation in the as-pressed grain size with the annealing temperature for pure Al after 4 passes using route B_C [26], an Al-3% Mg solid solution alloy after 8 passes using route B_C [26] and an Al-3% Mg-0.2% Sc alloy also after 8 passes using route B_C [27], where each experimental point relates to a separate as-pressed sample that was annealed for a total period of 1 h. It is apparent from Fig. 3 that the ultrafine grains produced by ECAP are not stable in pure Al and the Al-3% Mg alloy at temperatures above ~450 K whereas in the Al-Mg-Sc alloy there are Al_3Sc precipitates which provide reasonable grain stability, and an average grain size of <1 μm, up to temperatures of ~700 K.

Fig. 4 shows typical microstructures of these three materials in the as-pressed condition for (a) pure Al after 4 passes, (b) Al-3% Mg after 6 passes and (c) Al-3% Mg-0.2% Sc after 8 passes, together with appropriate selected area electron diffraction (SAED) patterns recorded from areas having diameters of 1.3 μm [28]. The measured grain sizes in these three materials are 1.3, 0.3 and 0.2 μm, respectively, thereby confirming an earlier report that smaller grain sizes are achieved in ECAP through alloying [29]. Furthermore, each of the SAED patterns exhibits rings which suggest that many of these boundaries have high angles of misorientation.

Fig. 5 shows an image produced using high-resolution electron microscopy (HREM) of the Al-3% Mg alloy after 6 passes in ECAP, where d_{111} denotes the {111} atomic planes in the lower grain [28]. The image in Fig. 5 depicts a triple junction at upper right and there are extrinsic dislocations along the grain boundaries marked by the letter "T" where each mark denotes the termination of an extra lattice plane on one side of the interface. The presence of these extrinsic dislocations in zones adjacent to the boundaries is consistent with extensive observations reported also for samples processed by HPT [30–32]. From these and other

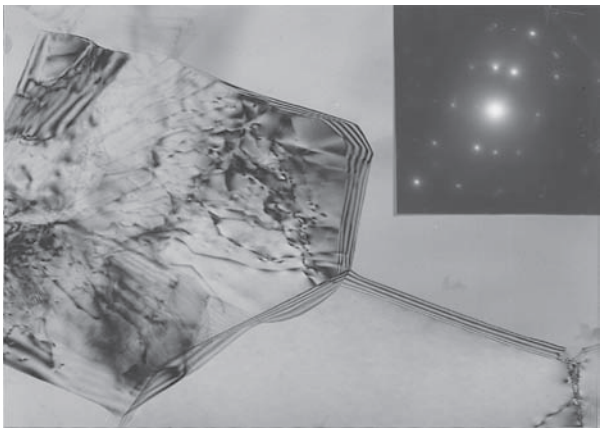

(a)

(b)

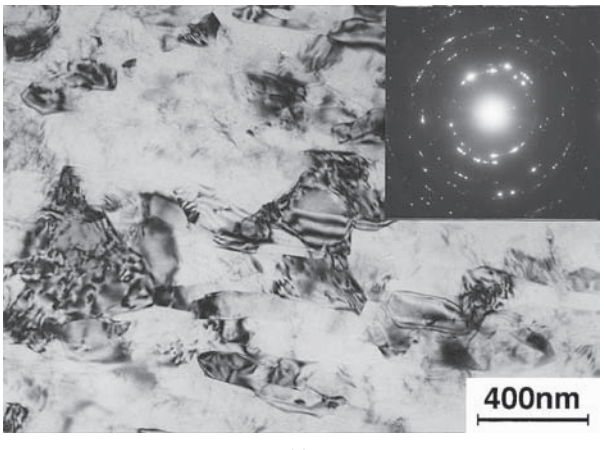

(c)

Figure 4 Typical microstructures after ECAP for (a) pure Al after 4 passes, (b) Al-3% Mg after 6 passes and (c) Al-3% Mg-0.2% Sc after 8 passes: the SAED patterns were recorded from areas having diameters of 1.3 μm [28].

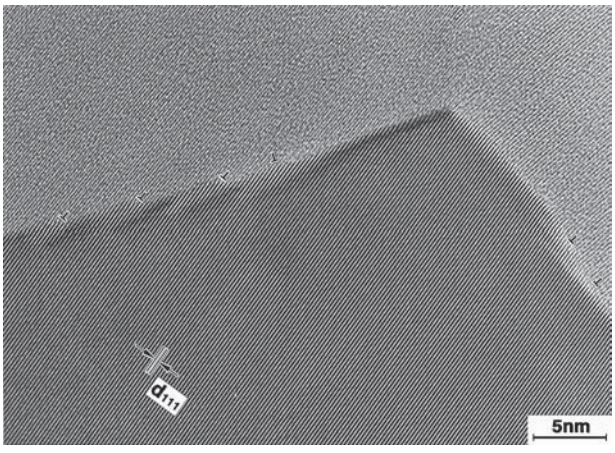

Figure 5 Structure in the vicinity of a triple point for an Al-3% Mg alloy after 6 passes of ECAP: extrinsic dislocations in the vicinity of the boundaries are marked by "T" [28].

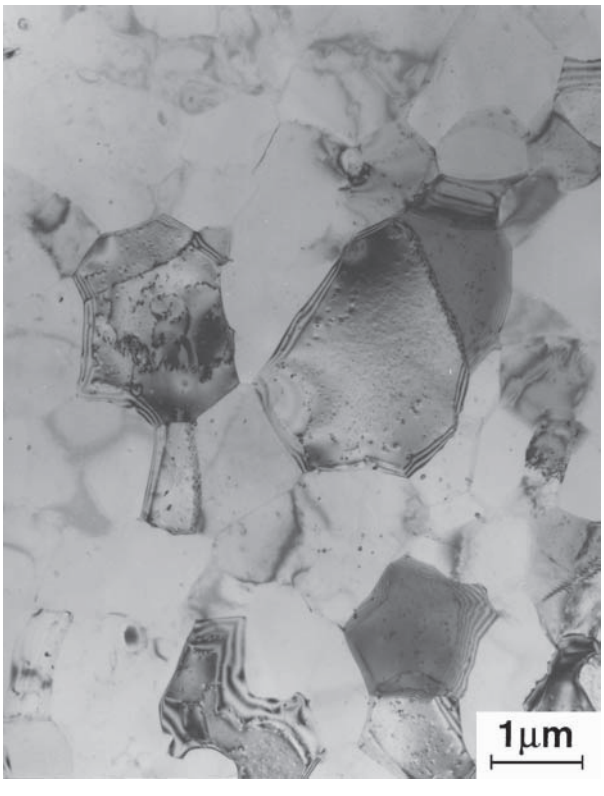

Figure 6 Microstructure in an Al-3% Mg-0.2% Sc alloy after 8 passes of ECAP and an anneal for 1 h at 673 K [28].

detailed observations conducted on samples after processing by ECAP [28, 33] and HPT [30–32], it has been concluded that the grain boundaries present in materials immediately after SPD processing are generally in a high-energy non-equilibrium configuration [34–36].

The microstructure in Fig. 6 was taken on the Al-Mg-Sc alloy after 8 passes of ECAP followed by an anneal for 1 h at 673 K [28]. Thus, despite the relatively high annealing temperature, the grain size is very small and of the order of $\sim$1 μm and the boundaries are now less curved and wavy than in the as-pressed condition shown in Fig. 4c. It is concluded that, although the annealing treatment has introduced some limited grain growth by a factor of $\sim 3\times$, there is also an evolution of the boundaries towards a more equilibrated structure. Close inspection of this material revealed the presence of both coherent and incoherent Al_3Sc particles in this condition [28].

4. Significance of ECAP in grain boundary engineering

Careful observations show that the microstructure introduced in ECAP gradually evolves towards a relatively homogeneous array of equiaxed grains separated by high-angle grain boundaries. This evolution is illustrated in Fig. 7 for samples of pure aluminum subjected

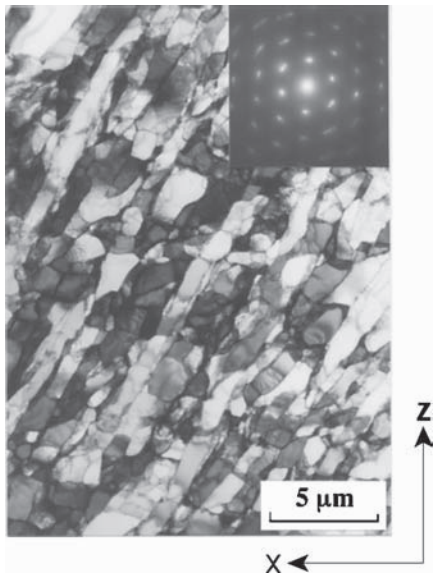

(a)

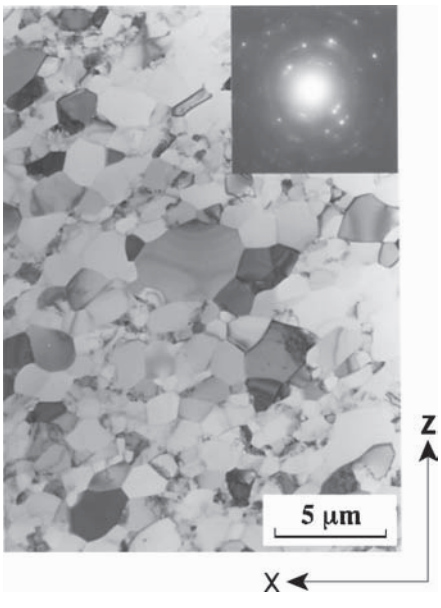

(b)

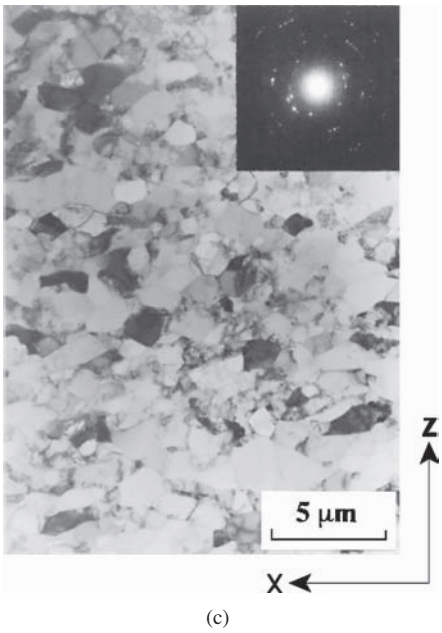

(c)

Figure 7 Microstructures in pure Al after ECAP through (a) 1 pass, (b) 4 passes and (c) 12 passes using processing route B_C: observations recorded on the Y plane [37].

to ECAP through (a) 1 pass, (b) 4 passes and (c) 12 passes using processing route B_C, where all observations were recorded on the Y plane [37]. A banded subgrain structure is clearly visible after 1 pass in Fig. 7a where these bands are closely aligned with the shear direction, but this microstructure evolves rapidly so that there is an array of essentially equiaxed grains after 4 passes in Fig. 7b and the shearing direction is no longer evident. Whereas the elongated subgrains in Fig. 7a have lengths of $\sim$4 μm in the shear direction and widths of $\sim$1.2 μm along the normal to the shear plane, the measured mean linear intercept grain size is $\sim$1.2 μm in Fig. 7b where it is noted that this is essentially equal to the subgrain width after a single pass. It is also apparent from the SAED patterns that there is an evolution in the boundary misorientations towards higher angles as the pressings continue to 4 passes. The equiaxed microstructure remains after 12 passes in Fig. 7c and the mean linear intercept grain size was then measured as $\sim$1.0 μm which suggests there may be a slight gradual refinement of the grain size with additional passes through the ECAP die. All of these results demonstrate the potential for using ECAP processing to achieve very substantial grain refinement even in materials, such as pure aluminum, where no precipitates are present to impede any movement of the grain boundaries.

The evolution in microstructure is evident also in the gradual increase in the fraction of high angle boundaries as recorded in Fig. 8 for these same samples subjected to 1, 4 and 12 passes, where high angle boundaries are defined as those having misorientations greater than 15° [37]. Measurements are shown in Fig. 8 for both the X and Y planes and the results suggest that $\sim$70% of the boundaries have high angles of misorientation after 12 passes with a slightly larger fraction visible on the X plane.

The results in Fig. 8 are consistent with other data reported for aluminum of slightly lower purity [38] but they are not consistent with experimental data for Cu subjected to 8 passes of ECAP where the fraction of high-angle boundaries was only $\sim$37% [39]. This difference probably arises because of the low stacking-fault energy in Cu and the consequent low

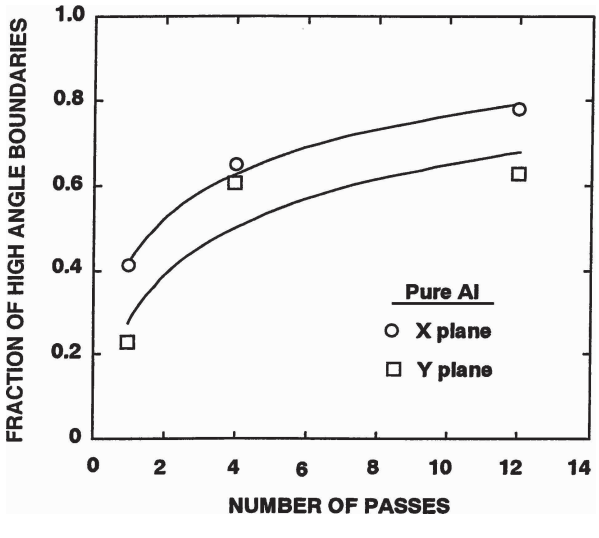

Figure 8 Fraction of high-angle boundaries on the X and Y planes in pure Al after ECAP through 1, 4 and 12 passes [37].

rate of recovery which is known to make it difficult to achieve a homogeneous structure during processing of this material by ECAP [40]. By contrast, the results for pure Al are consistent with those reported for pure Ni where the fractions of boundaries having high-angle misorientations were recorded as ~60% after ECAP through 8 passes and ~68% after processing by HPT [41]. Furthermore, the results on Ni are consistent with earlier observations on pure Ni showing that the stacking-fault energy of this material, which is intermediate between that of pure Al and pure Cu, leads to a smaller as-pressed grain size than in pure Al but a more homogeneous microstructure than in pure Cu [42]. Despite these relatively large fractions of high-angle boundaries, after either ECAP or HPT, it is important to note that there remains an excessively high proportion of low-angle boundaries for both processing techniques. This conclusion is based on calculations showing that a true random distribution of misorientation angles gives a fraction of 89.3% of high-angle boundaries having misorientations greater than 15° [43].

It is apparent from these observations that processing by ECAP provides two significant opportunities in the fabrication of materials with unusual properties. First, there is the well-established demonstration that ECAP leads to arrays of ultrafine grains that are typically in the submicrometer range and, even for pure metals where the grain sizes are close to ~1 μm, these sizes are much smaller than those achieved through conventional thermomechanical processing. Second, there is clear evidence for an evolution in the grain boundary character distributions from predominantly low-angle boundaries in the initial stages of ECAP to reasonably high fractions of high-angle boundaries ($\geq$60%) after large numbers of passes and consequently after the imposition of fairly high strains.

5. Influence of grain boundary character distribution on properties

An important paradox in materials science is that increases in strength are generally associated with corresponding decreases in ductility [44]. Accordingly, there is considerable current interest in developing thermomechanical processing procedures that lead to reasonable combinations of both high strength and good ductility: an example is given by recent experiments designed to produce a bimodal grain size distribution and consequent good tensile ductility in pure Cu [45]. An alternative approach is to tailor the microstructures produced through SPD processing in order to optimize the required properties [44]. The preceding section demonstrates that this latter approach may be developed to incorporate not only an ultrafine grain size in the processed material but also differences in the grain boundary character distributions during processing by ECAP. As demonstrated in this section, preliminary experiments show these distributions play an important role in dictating the behavior associated with both high temperature mechanical testing and the rate of diffusion. These two effects are now examined.

First, it is evident from Fig. 3 that the Al-3% Mg-0.2% Sc alloy exhibits exceptional microstructural stability even at temperatures close to 700 K. Since superplasticity is a diffusion-controlled process requiring tensile testing at a fairly high homologous temperature, it is reasonable to anticipate that the Al-Mg-Sc alloy will be an excellent candidate material for achieving high superplastic elongations. There is experimental evidence for exceptional ductility in this alloy when the material is processed by ECAP for a totals of 8 or 12 passes [27, 46–48] but in practice the extent of this ductility depends critically upon the number of passes through the die and therefore upon the imposed strain. This is illustrated in Fig. 9 where the upper specimen

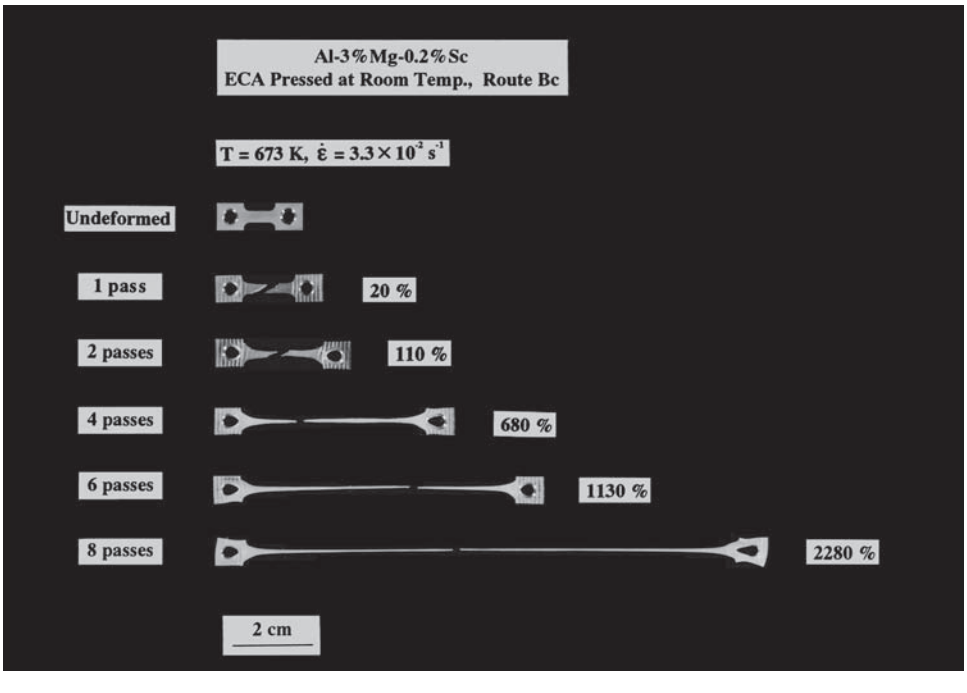

Figure 9 Variation of tensile ductility with number of passes in ECAP for an Al-3% Mg-0.2% Sc alloy pressed at room temperature using route B_C and then tested at 673 K with an initial strain rate of 3.3×10^{-2} s^{-1} [49].

is untested and the remaining specimens were pulled to failure at a temperature of 673 K using an initial strain rate of 3.3×10^{-2} s^{-1}: all samples were processed at room temperature using route B_C for totals from 1 to 8 passes and the measured elongations at the points of failure are indicated to the right of each sample [49]. It is apparent from these results that the ductility gradually increases with increasing numbers of passes through the ECAP die and this trend is a direct consequence of the need for easy grain boundary sliding in order to achieve superplastic elongations [50]. Thus, since low-angle boundaries exhibit little or no grain boundary sliding, the occurrence of superplasticity requires the presence of a reasonably high fraction of high-angle boundaries. It is reasonable to anticipate from Fig. 8 that ~60% of the boundaries in this alloy have high-angle misorientations after 8 passes and therefore grain boundary sliding occurs easily in this sample and the material pulls out uniformly to a total elongation in excess of 2000%. By contrast, the fraction of high-angle boundaries is insufficient to promote easy grain boundary sliding in the early stages of ECAP processing and the tensile elongations are then correspondingly reduced.

A second example relates to the influence of the grain boundary character distribution on diffusion. Fig. 10 shows the measured distribution of misorientation angles for an Al-3% Mg-0.2% Sc alloy subjected to ECAP at room temperature for 2 passes in route C and 8 passes in route B_C, respectively. As anticipated, there is a decrease in the number of low-angle boundaries and an increase in the number of high-angle boundaries as the material is taken through additional numbers of passes. Inspection of these measurements shows that approximately 58% of the boundaries have high misorientation angles after 8 passes through the die.

The diffusivities were measured separately in these samples of the Al-3% Mg-0.2% Sc alloy after 2 or 8 passes where the as-pressed grain size in both conditions was ~0.2 μm: for comparison purposes, additional measurements were taken also using a coarse unpressed alloy having a grain size of ~200 μm. Fig. 11 shows an Arrhenius plot of the experimental data recorded for the alloy in these three conditions [51] together with additional diffusion data for coarse-grained materials from other sources [52–56]. The values plotted in Fig. 11 correspond to the interdiffusion

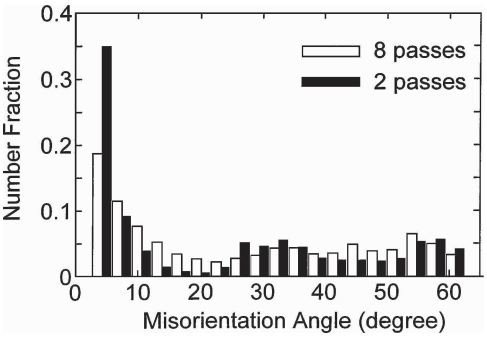

Figure 10 Number fraction of boundaries having different misorientation angles in an Al-3% Mg-0.2% Sc alloy after ECAP at room temperature through 2 and 8 passes.

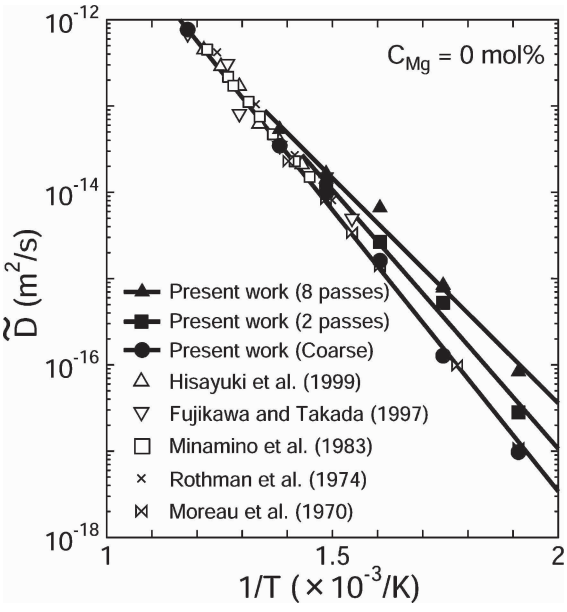

Figure 11 Arrhenius plot of the impurity diffusion coefficients for Mg in an Al lattice using data obtained from a coarse-grained sample, from samples subjected to ECAP through 2 and 8 passes [51] and from published data [52–56].

coefficient, $\tilde{D}$, versus the reciprocal of the absolute temperature, $1/T$, and they represent diffusion of Mg in an Al matrix at an extrapolated magnesium concentration, C_{Mg}, of 0%: in practice, therefore, they are equivalent to impurity diffusion coefficients. Inspection of Fig. 11 shows that the present data obtained on the coarse-grained alloy are consistent with the published data but the points for the two materials processed by ECAP lie along lines having lower slopes. In addition, the difference in the nature of the grain boundary distributions leads to a clear distinction between the data obtained on the alloy after 2 and 8 passes. For the coarse-grained material the activation energy for Mg diffusion in Al is estimated from Fig. 11 as ~126 kJ mol^{-1} whereas the activation energy is ~98 kJ mol^{-1} for the alloy after 8 passes [57] and there is an intermediate activation energy for the alloy after 2 passes. Since the diffusivity values for the alloy after 8 passes are significantly higher than for the coarse-grained material, these results provide a clear demonstration of the occurrence of rapid grain boundary diffusion in this ultrafine-grained material. Furthermore, the difference in slope in Fig. 11 between the samples processed through 2 and 8 passes provides confirmation that the grain boundary character distribution also plays an important role in these diffusivity measurements.

The two sets of results given in Figs 9 and 11 provide a clear illustration, for both high temperature mechanical properties and diffusion, that experimental data are critically dependent upon the nature of the grain boundary misorientations within the materials. There is a potential for achieving some control over the distributions of these misorientations when processing by ECAP since the internal structure gradually evolves with increasing strain from an array of boundaries having predominantly low-angles of misorientation to an array where there is a significant fraction of high-angle

boundaries. However, more work is now needed to critically evaluate the potential for tailoring the mechanical and physical properties through careful control of the total strain imposed in ECAP.

6. Summary and conclusions

1. Equal-channel angular pressing (ECAP) is a processing technique that is widely used to achieve considerable grain refinement, typically to the submicrometer level, in bulk polycrystalline materials. In addition, it is shown that the distribution of grain boundary misorientations in the as-processed material is a function of the total strain imposed in ECAP, with predominantly low-angle boundaries at low total strains but, at least for some materials, with a high fraction ($\geq$60%) of high-angle boundaries at high total strains.

2. This difference in misorientation distributions leads to significant effects when measurements are taken with as-pressed samples to determine properties such as the high temperature mechanical behavior or the rate of diffusion.

3. The development of these differences in the misorientation distributions provides a unique opportunity to utilize the ECAP process for grain boundary engineering and thus for developing and optimizing the beneficial properties in the as-pressed materials.

Acknowledgements

This work was supported in part by the Light Metals Educational Foundation of Japan, in part by the U.S. Army Research Office under Grant No. DAAD19-00-1-0488 and in part by the National Science Foundation of the United States under Grant No. DMR-0243331.

References

1. J. A. EWING and W. ROSENHAIN, *Proc. Roy. Soc*. A **65** (1899) 85.
2. D. McLEAN, "Grain Boundaries in Metals" (Clarendon Press, Oxford, England, 1957).
3. T. WATANABE, Res Mechanica **11** (1984) 47.
4. *Idem.*, *Key Eng. Mater*. **171–174** (2000) 237.
5. *Idem.*, *Mater. Sci. Forum* **408–412** (2002) 39.
6. T. WATANABE, H. FUJII, H. OIKAWA and K. I. ARAI, *Acta Metall*. **37** (1989) 941.
7. G. PALUMBO, P. J. KING, K. T. AUST, U. ERB and P. C. LICHTENBERG, *Scripta Metall. Mater*. **25** (1991) 1775.
8. D. C. CRAWFORD and G. S. WAS, *Metall. Trans*. A **32A** (1992) 1195.
9. T. WATANABE, Y. SUZUKI, S. TANII and H. OIKAWA, *Phil. Mag. Lett.* **62** (1990) 9.
10. T. WATANABE, in "Recrystallization and Grain Growth: Proceedings of the First Joint International Conference," edited by G. Gottstein and D. A. Molodov (Springer-Verlag, Berlin, Germany, 2001) p. 11.
11. R. Z. VALIEV, R. K. ISLAMGALIEV and I. V. ALEXANDROV, *Prog. Mater. Sci.* **45** (2000) 103.
12. T. C. LOWE and R. Z. VALIEV (eds.), "Investigations and Applications of Severe Plastic Deformation" (Kluwer, Dordrecht, The Netherlands, 2000).
13. V. M. SEGAL, V. I. REZNIKOV, A. E. DROBYSHEVSKIY and V. I. KOPYLOV, *Russian Metall*. **1** (1981) 99.
14. V. M. SEGAL, *Mater. Sci. Eng.* A **197** (1995) 157.
15. *Idem.*, *ibid.* A **271** (1999) 322.
16. M. FURUKAWA, Z. HORITA, M. NEMOTO and T. G. LANGDON, *J. Mater. Sci.* **36** (2001) 2835.
17. N. A. SMIRNOVA, V. I. LEVIT, V. I. PILYUGIN, R. I. KUZNETSOV, L. S. DAVYDOVA and V. A. SAZONOVA, *Fiz. Metal. Metalloved*. **61** (1986) 1170.
18. A. P. ZHILYAEV, G. V. NURISLAMOVA, B.-K. KIM, M. D. BARÓ, J. A. SZPUNAR and T. G. LANGDON, *Acta Mater.* **51** (2003) 753.
19. Z. HORITA, T. FUJINAMI and T. G. LANGDON, *Mater. Sci. Eng.* A **318** (2001) 34.
20. Y. IWAHASHI, J. WANG, Z. HORITA, M. NEMOTO and T. G. LANGDON, *Scripta Mater.* **35** (1996) 143.
21. M. FURUKAWA, Y. IWAHASHI, Z. HORITA, M. NEMOTO and T. G. LANGDON, *Mater. Sci. Eng.* A **257** (1998) 328.
22. M. FURUKAWA, Z. HORITA and T. G. LANGDON, *ibid.* A **332** (2002) 97.
23. K. OH-ISHI, Z. HORITA, M. FURUKAWA, M. NEMOTO and T. G. LANGDON, *Metall. Mater. Trans.* A **29A** (1998) 2011.
24. Y. IWAHASHI, Z. HORITA, M. NEMOTO and T. G. LANGDON, *Acta Mater*. **45** (1997) 4733.
25. *Idem.*, *ibid*. **46** (1998) 3317.
26. H. HASEGAWA, S. KOMURA, A. UTSUNOMIYA, Z. HORITA, M. FURUKAWA, M. NEMOTO and T. G. LANGDON, *Mater. Sci. Eng.* A **265** (1999) 181.
27. P. B. BERBON, S. KOMURA, A. UTSUNOMIYA, Z. HORITA, M. FURUKAWA, M. NEMOTO and T. G. LANGDON, *Mater. Trans. JIM* **40** (1999) 772.
28. K. OH-ISHI, Z. HORITA, D. J. SMITH and T. G. LANGDON, *J. Mater. Res.* **16** (2001) 583.
29. Y. IWAHASHI, Z. HORITA, M. NEMOTO and T. G. LANGDON, *Metall. Mater. Trans.* A **29A** (1998) 2503.
30. Z. HORITA, D. J. SMITH, M. FURUKAWA, M. NEMOTO, R. Z. VALIEV and T. G. LANGDON, *J. Mater. Res.* **11** (1996) 1880.
31. Z. HORITA, D. J. SMITH, M. NEMOTO, R. Z. VALIEV and T. G. LANGDON, *ibid.* **13** (1998) 446.
32. K. OH-ISHI, Z. HORITA, D. J. SMITH, R. Z. VALIEV, M. NEMOTO and T. G. LANGDON, *ibid.* **14** (1999) 4200.
33. J. WANG, Z. HORITA, M. FURUKAWA, M. NEMOTO, N. K. TSENEV, R. Z. VALIEV, Y. MA and T. G. LANGDON, *ibid.* **11** (1993) 2810.
34. R. Z. ABDULOV, R. Z. VALIEV and N. A. KRASILNIKOV, *J. Mater. Sci. Lett.* **9** (1990) 1445.
35. R. Z. VALIEV, N. A. KRASILNIKOV and N. K. TSENEV, *Mater. Sci. Eng.* A **137** (1991) 35.
36. R. Z. VALIEV, F. CHMELIK, F. BORDEAUX, G. KAPELSKI and B. BAUDELET, *Scripta Metall. Mater.* **27** (1992) 855.
37. S. D. TERHUNE, D. L. SWISHER, K. OH-ISHI, Z. HORITA, T. G. LANGDON and T. R. MCNELLEY, *Metall. Mater. Trans.* A **33A** (2002) 2173.
38. J.-Y. CHANG, J.-S. YOON and G.-H. KIM, *Scripta Mater.* **45** (2001) 347.
39. O. V. MISHIN, D. JUUL JENSEN and N. HANSEN, in "Recrystallization, Fundamental Aspects and Relations to Deformation Microstructure," edited by N. Hansen, X. Huang, D. Juul Jensen, E. M. Lauridsen, T. Leffers, W. Pantleon, T. J. Sabin and J. A. Wert (Risø National Laboratory, Roskilde, Denmark, 2000) p. 445.
40. S. KOMURA, Z. HORITA, M. NEMOTO and T. G. LANGDON, *J. Mater. Res.* **14** (1999) 4044.
41. A. P. ZHILYAEV, B.-K. KIM, G. V. NURISLAMOVA, M. D. BARÓ, J. A. SZPUNAR and T. G. LANGDON, *Scripta Mater.* **46** (2002) 575.
42. K. NEISHI, Z. HORITA and T. G. LANGDON, *Mater. Sci. Eng.* A **325** (2002) 54.
43. J. K. MACKENZIE, *Biometrika* **45** (1958) 229.
44. R. Z. VALIEV, I. V. ALEXANDROV, Y. T. ZHU and T. C. LOWE, *J. Mater. Res.* **17** (2002) 5.
45. Y. WANG, M. CHEN, F. ZHOU and E. MA, *Nature* **419** (2002) 912.

46. S. KOMURA, P. B. BERBON, M. FURUKAWA, Z. HORITA, M. NEMOTO and T. G. LANGDON, *Scripta Mater.* **38** (1998) 1851.
47. S. KOMURA, Z. HORITA, M. FURUKAWA, M. NEMOTO and T. G. LANGDON, *J. Mater. Res.* **15** (2000) 2571.
48. *Idem.*, *Metall. Mater. Trans.* A **32A** (2001) 707.
49. S. KOMURA, M. FURUKAWA, Z. HORITA, M. NEMOTO and T. G. LANGDON, *Mater. Sci. Eng.* A **297** (2001) 111.
50. T. G. LANGDON, *ibid.* A **174** (1994) 225.
51. T. FUJITA, Z. HORITA and T. G. LANGDON, *Mater. Sci. Forum* **396–402** (2002) 1061.
52. K. HISAYUKI, T. YAMANE, H. OKUBO, T. OKADA, T. TAKAHASHI and K. HIRAO, *Z. Metallkd.* **90** (1999) 423.
53. S. FUJIKAWA and Y. TAKADA, *Defect and Diffusion Forum* **143–147** (1997) 409.
54. Y. MINAMINO, Y. YAMANE, M. KOIZUMI, M. SHIMADA and N. OGAWA, *Z. Metallkd.* **73** (1982) 124.
55. S. J. ROTHMAN, N. L. PETERSON, L. J. NOWICKI and L. C. ROBINSON, *Phys. Stat. Sol.* (b) **63** (1974) K29.
56. G. MOREAU, J. A. CORNET and D. CALAIS, *J. Nucl. Mater.* **38** (1971) 197.
57. T. FUJITA, Z. HORITA and T. G. LANGDON, *Phil. Mag.* A **82** (2002) 2249.